J Polym Environ
DOI 10.1007/s10924-006-0033-4

ORIGINAL PAPER

Aromatic Copolyester-based Nano-biocomposites: Elaboration, Structural Characterization and Properties

Frédéric Chivrac · Zuzana Kadlecová · Eric Pollet · Luc Avérous

Abstract Biodegradable polymers are one of the most promising ways to replace non-degradable polymers. But, to be a real alternative to classical synthetic polymers and find applications, biopolymer (biodegradable polymer) properties have to be enhanced. Nano-biocomposites, which are obtained by incorporation of nanofillers into a biomatrix, are an interesting way to achieve these improvements. Modified and unmodified montmorillonites have been introduced into a biodegradable aromatic copolyester, poly(butylene adipate-*co*-terephthalate) (PBAT). Structural characterization, thermal and mechanical tests have been carried out to understand better the relations between the nanofillers structuring and the final nano-biocomposite properties. Main results show that clay incorporation and the obtained intercalated structures improve PBAT properties (enhanced thermal stability, increased stiffness) and thus may increase the attractiveness of this biopolymer.

Keywords Nano-biocomposites · Biodegradable polymer · Poly(butylene adipate-*co*-terephthalate) · Layered silicates · Montmorillonite

Introduction

Nowadays, most of the short-term application materials (e.g., packaging) are based on synthetic polymers. This situation is not entirely adequate because most of these long-lasting polymers produced from petrochemicals are not biodegradable and are a significant source of environmental pollution. Thus, reaching the conditions of conventional plastic replacements by degradable polymers is of major interest for different actors of the socio-economical life. However till now, biopolymers (biodegradable polymers) have not found extensive applications [1]. To be more attractive, some properties OF biopolymers have to be enhanced.

Preparations of blends or conventional composites are among the possible routes to improve polymers properties [2]. A new area of composites called nanocomposites, in which the reinforcing material has nanometric scale, has emerged and seems to be very promising. For instance, at low level of nanofillers incorporation (less than 5 wt%) [3–4], the reinforcement efficiency of nanocomposites can match that of conventional composites with 40–50 wt% of loading with classical fillers. This improvement is due to the dispersion of nanoscale fillers into the matrix, which results in a high surface area with high interactions between nanofillers and the polymer matrix.

The addition of nanofillers into a biodegradable polymer matrix leads to the creation of a novel class of materials, called nano-biocomposites which combine nano-materials with an environmental approach. Recent studies have been previously reported for the elaboration and characterization of these nano-materials, based on polylactide [5–7], poly(3-hydroxybutyrate)[8] and corresponding copolymers [9], plasticized starch [10–12], poly(butylene succinate) [13] or poly(ε-caprolactone) [14–18].

Various nano-reinforcements are currently under investigation. The most intensive researches concern

F. Chivrac · Z. Kadlecová · E. Pollet · L. Avérous (✉)
ECPM-LIPHT (UMR CNRS 7165), University Louis Pasteur, 25 rue Becquerel, F-67087 Strasbourg, Cedex 2, France
e-mail: AverousL@ecpm.u-strasbg.fr

Journal : 10924 | Dispatch : 1-8-2006 | Pages : 9
Article No. : 33 | ☐ LE | ☐ TYPESET
MS Code : 33 | ☑ CP | ☑ DISK

layered silicates as the reinforcing phase due to their availability, versatility and respectability towards the environment [19]. Enhanced thermal stability, improved gas barrier properties, increased stiffness or low melt viscosity are among the properties that can be achieved by these multiphase systems [20]. Montmorillonite (MMT) is a layered silicate commonly used in polymer nanocomposite preparation. It is a crystalline 2:1 layered clay mineral with a central alumina octahedral sheet sandwiched between two silica tetrahedral sheets [20]. These nanofillers have a hydrophilic character due to the presence of inorganic cations (Na^+, Ca^{2+}...) in the inter-layer spacing [21]. An ion-exchange reaction of intergallery inorganic cations with, for instance, alkyl ammonium cations can be carried out to promote the polymer–silicate compatibility.

Three main techniques can be used to prepare polymer/clay nanocomposites: melt intercalation, solvent intercalation and in situ polymerization [4]. In the first two techniques, the preformed polymer is mixed with the clay either in the molten state or in solution. In the third approach, clay is dispersed into the monomer solution which is further polymerised. The nanoparticles dispersed into the polymer matrix can be intercalated by macromolecules and/or exfoliated. Intercalated structures show regularly alternating layered silicates and polymer chains compared to exfoliated structures in which the individual clay layers are individually delaminated and fully dispersed in the polymer matrix. Best performances (mechanical and physical properties) are commonly observed with the exfoliated structures.

Recently, Someha et al. [22] have published on the analysis of nano-biocomposites based on poly(butylene adipate-*co*-terephthalate) (PBAT) and layered silicates they have themselves organomodified. PBAT is a synthetic copolyester obtained from fossil resources and known to be biodegradable. The degradation mechanism of this biopolymer has been investigated by both the study of the hydrolytic and the enzymatic degradation [23, 24]. These studies have demonstrated that the biodegradation rate mainly depend on the adipate content of this bio-copolyester. The present article completes and expands the Someha's work. It is focussed on the elaboration and characterization of PBAT nano-biocomposites prepared by both solvent and melt intercalation with different kind of commercial organo-modified montmorillonites. Structural, thermal and mechanical properties have been studied as a function of the preparation method as well as the content and nature of clay to understand better the relations between the nanofillers structuring and the final nano-biocomposite properties.

Experimental Part

Materials

The matrix is a biodegradable aromatic copolyester PBAT, which has been kindly supplied by Eastman (EASTAR BIO Ultra Copolyester 14766). Figure 1 shows PBAT chemical structure. Figure 2 shows the ^1H NMR spectrum of PBAT, dissolved in $CDCl_3$. The ratio between each monomer unit has been determined by ^1H NMR. The integration of the peaks of the adipate unit (BA) and the terephthalate unit (BT), respectively at 2.33 ppm and 8.1 ppm, gives PBAT composition: 57% of BA and 43% of BT. Determined by size exclusion chromatography (SEC), average molecular weight (M_w) and polydispersity index (I) are 48,000 g mol^{-1} and 2.4, respectively. Melt flow index (MFI) is 13 g/10 min at 190 °C/2.16 kg. Density is 1.27 g/cm^3 at 23 °C.

The clay minerals studied were kindly supplied by Southern Clay Products, Inc. (Cloisite® 20A), Laviosa Chimica Mineraria S.p.A. (Dellite® LVF, Dellite® 43B) and Süd-Chemie (Nanofil® 804). The unmodified montmorillonite is Dellite® LVF (MMT-Na). The three organo-modified montmorillonites are Cloisite® 20A (OMMT-Alk) which is organo-modified by dimethyl dihydrogenated tallow ammonium, Dellite® 43B (OMMT-Bz) which is organo-modified with benzyl dimethyl hydrogenated tallow ammonium and Nanofil® 804 (OMMT-$(OH)_2$) which is organo-modified by dihydroxyethyl methyl tallow ammonium. As determined by thermogravimetric analysis (TGA), organic contents are 31.0 wt%, 8.0 wt% and 30.5 wt% for OMMT-Alk, OMMT-Bz and OMMT-$(OH)_2$, respectively. Organo-modifiers chemical structures are given in Fig. 3.

Nano-biocomposites Elaboration

Before processing, PBAT and clays were dried overnight at 80 °C under reduced pressure. To obtain nano-biocomposites, from 3 wt% to 9 wt% of MMT have been added into PBAT matrix according to two synthetic routes: solvent or melt intercalation.

Solvent Intercalation

The nano-biocomposites were prepared by solvent intercalation in chloroform. About 700 mg of PBAT are introduced into 35 mL of $CHCl_3$ at 50 °C and sonicated until solubilisation. Then, the adequate amount of MMT is introduced into the mixture and sonicated at 50 °C for 4 h. Finally, the solution is

Journal : 10924 | Dispatch : 1-8-2006 | Pages : 9
Article No. : 33 | ☐ LE | ☐ TYPESET
MS Code : 33 | ☑ CP | ☑ DISK

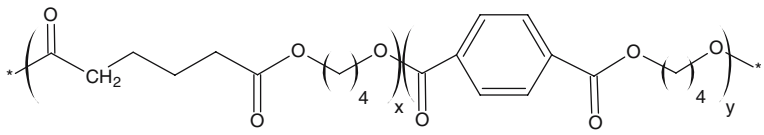

Fig. 1 Chemical structure of poly(butylene adipate-*co*-terephthalate)

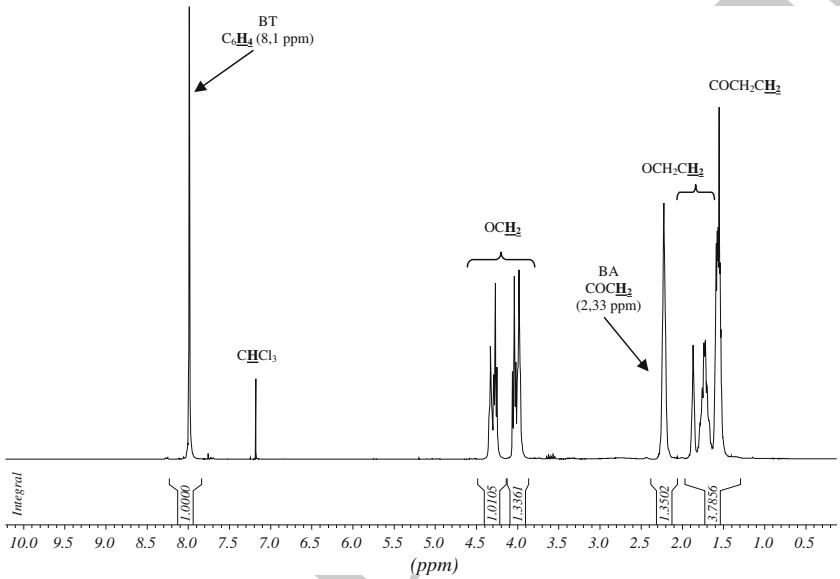

Fig. 2 ^{1}H NMR spectrum of PBAT

poured into a petri dish and nano-biocomposites films are obtained by solvent casting under atmospheric conditions, at ambient temperature for 24 h.

Melt Intercalation

The nano-biocomposites were prepared by mechanical kneading with an internal batch mixer, a counter-rotating mixer Rheocord 9000 (Haake-USA), at 160 °C for 15 min with a rotor speed of 50 rpm followed by another step at 120 °C for 20 min with a rotor speed of 100 rpm. After melt processing, the molten materials were compression-molded to obtain films with a hot press at 160 °C applying 20 MPa pressure for 10 min. The molded specimens were quenched between two steel plates for 3 min to allow the specimens to be fully crystallized before testing.

Characterization

SEC and ^{1}H NMR Measurements

SEC measurements were performed in THF (HPLC grade), with PS standards for the calibration, on a Shimadzu LC-10AD liquid chromatograph (Japan) equipped with a Shimadzu RID-10A refractive index detector and a Shimadzu SPP-M10A diode array UV detector. ^{1}H NMR spectra were recorded in $CDCl_3$ on a Bruker 300 UltrashieldTM 300 MHz (Germany).

XRD Characterization

The X-Ray Diffraction (XRD) morphological analyses were performed on a powder diffractometer Siemens D 5000 (Germany) using Cu (Kα) radiation (wavelength:

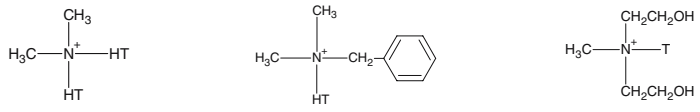

OMMT-Alk OMMT-Bz OMMT-$(OH)_2$

Fig. 3 Chemical structures of the organo-modifiers

T = Tallow (~65% C18; ~30% C16; ~5% C14)

HT = Hydrogenated Tallow

Journal : 10924 Dispatch : 1-8-2006 Pages : 9
Article No. : 33 LE TYPESET
MS Code : 33 CP DISK

1.5406 Å) at room temperature in the range of $2\theta = 1.5$ to 30° by step of 0.03° of 1s, each.

TEM Analysis

For TEM observation, the samples were microtomed at low temperature (–55 °C) using a Leica Ultracut S cryo-microtome (Japan) equipped with a diamond knife. The ultra thin sections (ca. 40 nm, prepared from 3 mm thick plates) were examined using a Philips CM 12 (Netherland) transmission electron microscope using an acceleration voltage of 120 kV.

DSC Characterization

The thermal behaviours of PBAT and its nano-biocomposites were analyzed by Differential Scanning Calorimetry (DSC) using a DSC 2910 apparatus from TA Instrument (USA). The analyses were performed on 5–10 mg samples, at a heating rate of 10 °C/min from –70 °C to 200 °C. The reported values were recorded during the second heating scan. The glass temperature (T_g) is measured at the maximum of the derivative of the heat flow signal when the ΔC_p gap occurs. The melting temperature (T_m) is measured from the maximum of the endothermic peak. The melting enthalpy (ΔH_m) is measured from the area of the endothermic peak and has been corrected from a dilution effect using the Eq. (1), where x is the percentage of organic content, ΔH_{m_0} is the initial melting enthalpy and ΔH_m the corrected melting enthalpy.

$$\Delta H_m = \Delta H_{m_0} * \frac{100}{x} \quad (1)$$

The degree of crystallinity (χ) is estimated from Eq. 2, where ΔH_m is the corrected enthalpy of nano-biocomposites based on PBAT and $\Delta H_{m_{100}}$ is the theoretical enthalpy of 100% crystalline PBAT.

$$\chi = \frac{\Delta H_m}{\Delta H_{m_{100}}} * 100 \quad (2)$$

$\Delta H_{m_{100}}$ has been determined following the approach presented by Herrera et al. [23] $\Delta H_{m_{100}}$ is calculated by the contribution of the different chain groups. The contributions of ester, methylene and *p*-phenylene groups are –2.5 kJ/mol, 4.0 kJ/mol and 5.0 kJ/mol, respectively. The calculated values ($\Delta H_{m_{100}}$) is equal to 22.3 kJ/mol, i.e. 114 J/g. From this value, the degree of crystallinity of PBAT has been determined.

TGA Characterization

All thermogravimetric analyses (TGA) were performed on 5–15 mg samples, at a heating rate of 20 °C/min from 25 to 600 °C on a Hi-Res TGA 2950 apparatus from TA Instruments (USA). For all PBAT/clay nano-biocomposites, the analyses were carried out under ''synthetic air,'' which is a mixture of 75% N_2 and 25% O_2. The clay content in inorganics (in wt%) of each composite was assessed by TGA as the combustion residue left at 600 °C. The organic content (in wt%) of the organo-modified clay was determined by the weight loss recorded between 150 °C and 450 °C, corresponding to the ammonium cations thermal degradation. The degradation temperature is determined from the peak temperature of the derivative weight loss curve.

Mechanical Tests

Tensile tests were carried out with an Instron tensile testing machine (model 4204, USA), at 25 °C with a constant deformation rate of 10 mm/min, according to the ASTM D882-91 norm. Samples were dumbbell-shaped specimens prepared by injection molding (160 °C, 100 Mpa) with a Minijet from ThermoHaake (USA). Ten samples for each formulation were tested. The non-linear mechanical behaviour of the different samples was determined through different parameters. The true strain is given by Eq. (3). In this equation, L and L_0 are the length during the test and at zero time. Two different strains were calculated; strain at the yield point (ε_y) and at break (ε_b).

$$\varepsilon = \ln\left(\frac{L}{L_0}\right) \quad (3)$$

The nominal stress was determined by Eq. (4), where F is the applied load and S_0 is the initial cross-sectional area. The true stress was given by Eq. (5), where F is the applied load and S is the cross-sectional area. S was estimated assuming that the total volume of the sample remained constant, according to Eq. (6). The estimation of S is strictly valid before striction and has no physical meaning after. Both, stress at the yield point (σ_y) and at break (σ_b) are determined. σ_y is estimated with the true stress value and σ_b is determined with the nominal stress value (because of the striction).

$$<\sigma> = \frac{F}{S_0} \quad (4)$$

Journal : 10924 | Dispatch : 1-8-2006 | Pages : 9
Article No. : 33 | LE | TYPESET
MS Code : 33 | CP | DISK

$$\sigma = \frac{F}{S} \quad (5)$$

$$S = S_0 * \frac{L_0}{L} \quad (6)$$

Young's modulus (E) was measured from the slope of the low strain region in the vicinity of 0 ($\sigma = \varepsilon = 0$).

Results and Discussion

Structural Characterization

XRD Characterization

Figure 4 shows typical XRD patterns recorded for pristine PBAT, OMMT-Alk organoclay and PBAT/OMMT-Alk nano-biocomposites. Five diffraction peaks of the PBAT crystal structure are observed at 2θ angle 16.4°, 17.4°, 20.6°, 22.8° and 24.7°, respectively. These five characteristic peaks are also observed at the same values for all PBAT nano-biocomposites. Consequently, these results suggest that there are no important transcrystallinity at the nanofillers/PBAT interface and thus, few or no change in the PBAT crystal structure induced by nanofillers incorporation. A decrease of the intensity of these diffraction peaks is observed when clay loading increases, indicating a drop in the PBAT crystallinity. Thus, it seems that the nanofillers likely hinder the crystal growth of PBAT crystallite.

The OMMT-Alk diffraction pattern displays two diffraction peaks at low 2θ angles (4.1 and 7.9) corresponding to the d_{001} and d_{002} values, respectively. The clay inter-layer spacing is calculated from the d_{001} peak using the Bragg's law. Table 1 summarizes the inter-layer spacing results for different nano-biocomposites prepared with MMT-Na, OMMT-Alk, OMMT-Bz and OMMT-$(OH)_2$ obtained by solvent and melt intercalation. It was impossible to obtain nano-biocomposites from solvent intercalation with MMT-Na and OMMT-$(OH)_2$, because these two nanofillers sediment in chloroform.

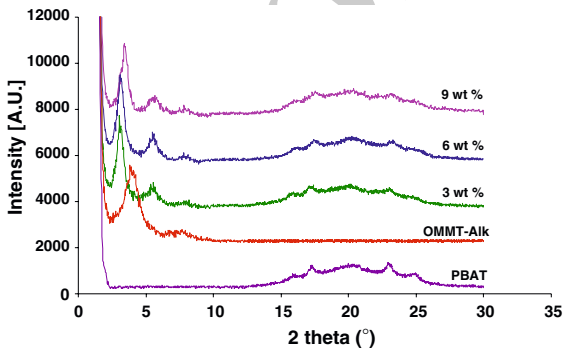

Fig. 4 Typical XRD patterns of PBAT/OMMT-Alk nano-biocomposites

Table 1 Inter-layer spacing values for the pristine MMT and their respective PBAT nano-biocomposites

	Samples	D_{001} (Å)
Nanofillers	MMT-Na	12.1
	OMMT-Alk	21.8
	OMMT-Bz	32.7
	OMMT-$(OH)_2$	18.5
Solvent intercalation	PBAT/OMMT-Alk 3 wt%	38.5
	PBAT/OMMT-Alk 6 wt%	36.3
	PBAT/OMMT-Alk 9 wt%	35.7
	PBAT/OMMT-Bz 3 wt%	37.4
	PBAT/OMMT-Bz 6 wt%	36.8
	PBAT/OMMT-Bz 9 wt%	36.6
Melt intercalation	PBAT/MMT-Na 3 wt%	25.1
	PBAT/MMT-Na 6 wt%	24.7
	PBAT/MMT-Na 9 wt%	23.9
	PBAT/OMMT-Alk 3 wt%	29.8
	PBAT/OMMT-Alk 6 wt%	28.8
	PBAT/OMMT-Alk 9 wt%	26.4
	PBAT/OMMT-Bz 3 wt%	28.5
	PBAT/OMMT-Bz 6 wt%	28.5
	PBAT/OMMT-Bz 9 wt%	26.7
	PBAT/OMMT-$(OH)_2$ 3 wt%	29.1
	PBAT/OMMT-$(OH)_2$ 6 wt%	28.3
	PBAT/OMMT-$(OH)_2$ 9 wt%	27.9

For all the PBAT nano-biocomposites samples, an intense d_{001} diffraction peak is observed meaning that these materials are mostly intercalated and not fully exfoliated. Table 1 shows that samples prepared from solvent intercalation present an increase of the inter-layer spacing, thus suggesting an effective intercalation of PBAT chains. Inter-layer spacing values observed for nano-biocomposites prepared with OMMT-Alk and OMMT-Bz are equivalent, which probably means that these two nanofillers have an equivalent affinity with PBAT.

Except for the PBAT/OMMT-Bz samples, results obtained from melt intercalation show an increase of the inter-layer spacing. This means that there is intercalation of PBAT chains into montmorillonite inter-layer spacing. However, we can notice lower polymer intercalations compared to those obtained by solvent intercalation. An interesting point is the increase of intergallery spacing observed for nano-biocomposites prepared with MMT-Na. This result demonstrates that intercalated nanocomposites can be obtained with PBAT even without organo-modifying the nanofillers. Equivalent results had been obtained on plasticized starch [10–12]. But, non-modified montmorillonite

Journal : 10924 Dispatch : 1-8-2006 Pages : 9
Article No. : 33 LE TYPESET
MS Code : 33 CP DISK

melt-blended with polyesters usually leads to micro-composites [3].

TEM

Figure 5 shows typical TEM micrographs of the PBAT/OMMT nano-biocomposites stemmed from melt intercalation containing 3 wt% of OMMT-Alk. Since silicate layers are composed of heavier elements (Al, Si, Mg) than surrounding matrix (C, H, N and O), they appear darker in the bright-field images. The micrographs show that the montmorillonite layers are not homogeneously dispersed. TEM results confirm that PBAT-based nano-biocomposites mainly display an intercalated structure on agreement with XRD analyses. Evaluated from the micrographs, the average distance between clay layers is found to be around 30 Å which is in good agreement with the inter-layer spacing results obtained from XRD analyses.

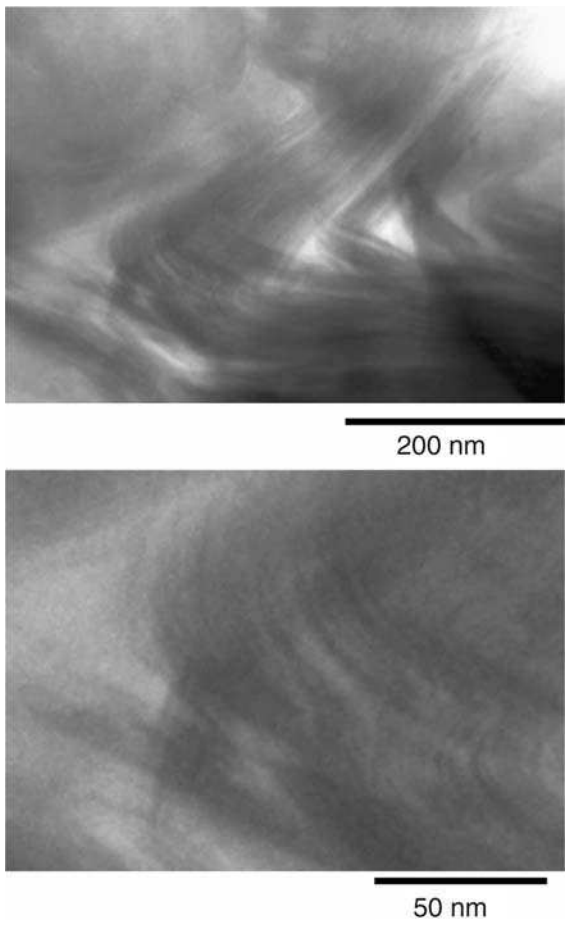

Fig. 5 TEM picture of a PBAT/OMMT-Alk 3 wt% nano-biocomposite obtained by melt intercalation

Thermal Properties

DSC

Table 2 summarizes the results obtained by DSC measurements. According to these measurements, PBAT glass temperature (T_g) is –38 °C, PBAT melting temperature (T_m) is 110 °C and crystallinity degree (χ) is around 10.8%. On one hand, the nano-biocomposites glass temperature (T_g) values seem to indicate that nanofillers have no effect on glass transition. Similarly, the nano-biocomposite melting temperatures (T_m) are closed to neat PBAT melting temperature. These results agree with XRD analyses indicating that nanofiller addition does not change PBAT crystal organization. On the other hand, the melting enthalpy (ΔH_m) and therefore the crystallinity (χ) are affected by clay addition. Compared to neat PBAT, the variations observed at 3 wt% are not significant, but drops of χ are observed when clay content increases towards 9 wt%. This result also agrees with XRD analyses, and seems to indicate that nanofillers hinder the PBAT crystallite growth.

TGA

The thermal stability is assessed by thermogravimetric analysis (TGA). Figure 6 shows typical TGA thermograms obtained for neat PBAT and the corresponding nano-biocomposites proceed from melt intercalation. Table 3 presents the nano-biocomposite degradation temperatures. PBAT degradation temperature is 395 °C. The nano-biocomposite degradation temperatures are higher or at least equal to PBAT one. The highest improvements are observed for nano-biocomposites filled with 3 wt% of montmorillonite and a decrease of the degradation temperature is observed for higher clay contents, both with melt and solvent intercalations. This behaviour is in agreement with published results obtained on polyester/montmorillonite nanocomposites [20]. The highest degradation temperatures are observed for PBAT/MMT-Na nano-biocomposites.

It is widely accepted [3, 25–28] that layered silicates enhance the thermal stability of the polymer matrix because they act as a heat barrier, which enhances the overall thermal stability of the system, as well as assists in the formation of char during thermal decomposition. Nevertheless, only a slight improvement is observed for PBAT nano-biocomposites. To explain this rather low thermal stability improvement with some nano-composite systems, Sinha Ray and Okamato [20] have

Journal : 10924 Dispatch : 1-8-2006 Pages : 9
Article No. : 33 LE TYPESET
MS Code : 33 CP DISK

Table 2 Thermal properties of PBAT nano-biocomposites measured by DSC

Preparation method	Samples	T_g (°C)	T_m (°C)	ΔH_m (J/g)	χ (%)
–	PBAT	– 38	110	12.3	10.8
Solvent intercalation	PBAT/OMMT-Alk 3 wt%	– 38	111	12.6	11.1
	PBAT/OMMT-Alk 6 wt%	– 38	111	12.5	11.0
	PBAT/OMMT-Alk 9 wt%	– 38	111	12.1	10.6
	PBAT/OMMT-Bz 3 wt%	– 37	111	11.4	10.0
	PBAT/OMMT-Bz 6 wt%	– 37	111	11.2	9.8
	PBAT/OMMT-Bz 9 wt%	– 37	111	10.9	9.6
Melt intercalation	PBAT/MMT-Na 3 wt%	– 37	111	13.2	11.6
	PBAT/MMT-Na 6 wt%	– 37	111	11.0	9.6
	PBAT/MMT-Na 9 wt%	– 38	112	11.4	10.0
	PBAT/OMMT-Alk 3 wt%	– 37	110	10.2	8.9
	PBAT/OMMT-Alk 6 wt%	– 37	111	10.3	9.0
	PBAT/OMMT-Alk 9 wt%	– 37	111	10.0	8.8
	PBAT/OMMT-Bz 3 wt%	– 37	111	11.6	10.2
	PBAT/OMMT-Bz 6 wt%	– 37	112	10.6	9.3
	PBAT/OMMT-Bz 9 wt%	– 36	113	10.4	9.1
	PBAT/OMMT-$(OH)_2$ 3 wt%	– 38	111	12.0	10.5
	PBAT/OMMT-$(OH)_2$ 6 wt%	– 38	111	10.2	8.9
	PBAT/OMMT-$(OH)_2$ 9 wt%	– 38	111	9.3	8.2

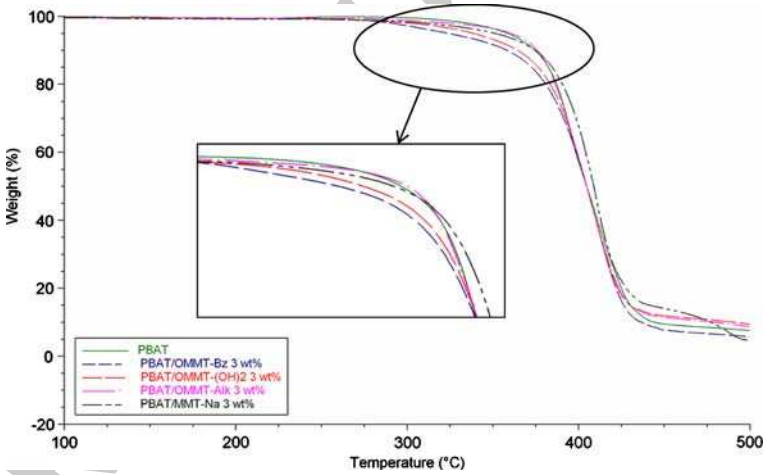

Fig. 6 Typical thermograms (weight loss vs. temperature) obtained under ''synthetic air'' flow for PBAT, PBAT/MMT-Na 3 wt%, PBAT/OMMT-Alk 3 wt%, PBAT/OMMT-$(OH)_2$ 3 wt% and PBAT/OMMT-Bz 3 wt% stemmed from melt intercalation

recently assumed that in the early stages of thermal decomposition, the clay would shift the decomposition to higher temperature. But in a second step, the clay layers could accumulate heat and then be transformed as a heat source and promote an acceleration of the decomposition process in combination with the heat flow supplied by the outside heat source. That could explain why in our case there is only a slight improvement of the thermal degradation temperatures.

Mechanical Properties

Tensile tests have been carried out on nano-biocomposite samples prepared from melt intercalation.

Table 3 Degradation temperatures of PBAT and its nano-biocomposites

Preparation method	Samples	Degradation temperature (°C)
–	PBAT	395
Solvent intercalation	PBAT/OMMT-Alk 3 wt%	405
	PBAT/OMMT-Alk 6 wt%	403
	PBAT/OMMT-Alk 9 wt%	395
Melt intercalation	PBAT/MMT-Na 3 wt%	410
	PBAT/MMT-Na 6 wt%	408
	PBAT/MMT-Na 9 wt%	405
	PBAT/OMMT-Alk 3 wt%	406
	PBAT/OMMT-Alk 6 wt%	395
	PBAT/OMMT-Alk 9 wt%	394
	PBAT/OMMT-Bz 3 wt%	411
	PBAT/OMMT-$(OH)_2$ 3 wt%	407

Journal : 10924 Dispatch : 1-8-2006 Pages : 9
Article No. : 33 LE TYPESET
MS Code : 33 CP DISK

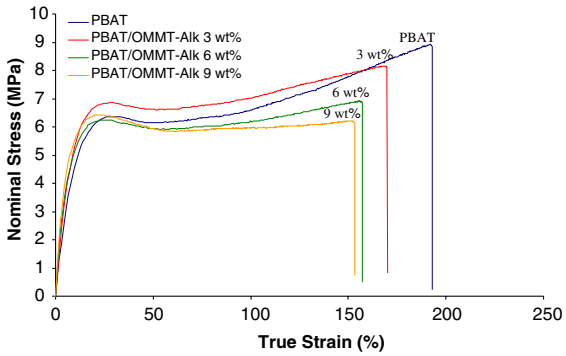

Fig. 7 Typical tensile curves obtained for neat PBAT and PBAT/OMMT-Alk 3, 6 & 9 wt%

Figure 7 presents the typical tensile curves obtained for PBAT/OMMT-Alk 3, 6 and 9 wt%. Table 4 summarizes the Young's modulus (E) and other mechanical properties of PBAT and nano-biocomposites. According to these mechanical tests, PBAT Young's modulus (E) is 57 MPa, strain at yield (ε_y) is 28%, strain at break (ε_b) is 188%, stress at yield (σ_y) is 8.1 MPa and stress at break (σ_b) is 55 MPa. The addition of nanofillers leads to substantial improvement in stiffness correlated to the increase in clay loading, even if there is a decrease of the PBAT crystallinity observed by both DSC and XRD. Consequently, the observed increase in rigidity is induced by the nanofiller incorporation into the matrix and stem from strong interactions between nanofillers and PBAT chains. However, there are notable differences in the level of improvement between PBAT/MMT-Na and PBAT/OMMT-Alk. The stronger affinity of organo-modified montmorillonites with PBAT leads to a better dispersion and stronger interactions resulting in a higher Young's modulus. The addition of clay leads to a decrease in the strain at yield (ε_y) and at break (ε_b) values. These drops are correlated with the clay content and are more pronounced for unmodified montmorillonite. The decrease of stress at break (σ_b) observed for all nano-biocomposites samples when clay loading increases is likely linked to nanofillers dispersion. The addition of nanofillers does not really change the stress at yield, except for PBAT/MMT-Na 9 wt%. This poor value is probably induced by the lower affinity of PBAT for MMT-Na.

Conclusions

The aim of this study was the elaboration of nano-biocomposites by two methods: solvent and melt intercalation. Structural, thermal and mechanical characterizations were performed to understand better the relations between the preparation routes, nanofillers structuring and the final nano-biocomposites properties. For both elaboration techniques, intercalated nano-biocomposites were obtained. This nanostructure was pointed out by both XRD analyses and TEM observations. Higher intercalation levels have been obtained for samples prepared from solvent intercalation compared to those obtained by melt intercalation. No significant change induced by the nanofillers incorporation has been observed by XRD on the PBAT crystal structure. Both XRD and DSC analyses have evidenced a decrease in the PBAT crystallinity induced by the clay incorporation, probably because nanofillers hinder crystallite growth. The DSC results have shown that the nanofillers have no significant influence on the biopolymer T_g and T_m. An improvement of PBAT thermal stability has been noticed by TGA, mainly at low clay content (3 wt%). Tensile tests have shown that the nano-biocomposites stiffness increases continuously with clay content. Nevertheless, a decrease in the strain at yield (ε_y) and at break (ε_b) has been observed.

Therefore, all results presented here clearly demonstrate that the appropriate incorporation of montmorillonite as a nanofiller can improve PBAT properties and thus increase the attractiveness of this biodegradable polymer. Indeed, these nano-biocomposites materials are on agreement with the emergent concept of sustainable development.

Table 4 Mechanical properties (calculated from the stress-strain curves) of PBAT nano-biocomposites prepared by melt-intercalation

Samples	E (MPa)	ε_y (%)	ε_b (%)	σ_y (MPa)	σ_b (MPa)
PBAT	57 ± 3	28 ± 1	188 ± 15	8.1 ± 0.4	55 ± 11
PBAT/MMT-Na 3 wt%	66 ± 4	26 ± 3	128 ± 22	8.4 ± 0.3	26 ± 6
PBAT/MMT-Na 6 wt%	81 ± 4	20 ± 1	120 ± 15	8.3 ± 0.4	23 ± 4
PBAT/MMT-Na 9 wt%	88 ± 4	15 ± 4	59 ± 8	6.7 ± 1.5	11 ± 1
PBAT/OMMT-Alk 3 wt%	72 ± 2	26 ± 2	172 ± 7	8.1 ± 0.3	42 ± 4
PBAT/OMMT-Alk 6 wt%	84 ± 4	23 ± 2	163 ± 7	8.5 ± 0.3	36 ± 4
PBAT/OMMT-Alk 9 wt%	111 ± 3	21 ± 2	144 ± 8	8.6 ± 0.5	27 ± 2

Journal : 10924 Dispatch : 1-8-2006 Pages : 9
Article No. : 33 LE TYPESET
MS Code : 33 CP DISK

Acknowledgments The authors thank the IPCMS (Institut de Physique et Chimie des Matériaux et du Solide) and the ICS (Institut Charles Sadron) in Strasbourg (France) for their technical support. Thanks are also extended to Dr. Christian Chaumont and Perrine Bordes (ECPM-Strasbourg) for their technical insight.

References

1. Avérous L (2004) J Macromol Sci Pt C-Polym Rev C44:231
2. Le Digabel F, Boquillon N, Dole P, Monties B, Avérous L (2004) J Appl Polym Sci 93:428
3. Alexandre M, Dubois P (2000) Mater Sci Eng R 28:1
4. Pinnavaia TJ, Beall GW (2000) Polymer–clay nanocomposites. Wiley, New-York
5. Ogata N, Jimenez G, Kawai H, Ogihara T (1997) J Polym Sci Pt B-Polym Phys 35:389
6. Bandyopadhyay S, Chen R, Giannelis EP (1999) Polym Mater Sci Eng 81:159
7. Ray SS, Yamada K, Okamoto M, Ueda K (2002) Nano Lett 2:1093
8. Maiti P, Batt CA, Giannelis EP (2003) Polym Mater Sci Eng 88:58
9. Chen GX, Hao GJ, Guo TY, Song MD, Zhang BH (2004) J Appl Polym Sci 93:655
10. de-Carvalho AJF, Curvelo AAS, Agnelli JAM (2001) Carbohydr Polym 45:189
11. Park HM, Lee WK, Park CY, Cho WJ, Ha CS (2003) J Mater Sci 38:909
12. Park HM, Li X, Jin CZ, Park CY, Cho WJ, Ha CK (2002) Macromol Mater Eng 287:553
13. Ray SS, Okamoto K, Maiti P, Okamoto M (2002) J Nanosci Nanotechnol 2:171
14. Pantoustier N, Alexandre M, Degee P, Calberg C, Jerome R, Henrist C (2001) e-Polymer 9:1
15. Pantoustier N, Lepoittevin B, Alexandre M, Kubies D, Calberg C, Jerome R (2002) Polym Eng Sci 42:1928
16. Lepoittevin B, Devalckenaere M, Pantoustier N, Alexandre M, Kubies D, Calberg C (2002) Polymer 43:4017
17. Viville P, Lazzaroni R, Pollet E, Alexandre M, Dubois P, Borcia G, Pireaux JJ (2003) Langmuir 19:9425
18. Gain O, Espuche E, Pollet E, Alexandre M, Dubois P (2005) J Polym Sci Pt B-Polym Phys 43:205
19. Okamoto M (2004) J Ind Eng Chem 10:1156
20. Ray SS, Okamoto M (2003) Prog Polym Sci 28:1539
21. Grim RE (1953) Clay mineralogy. McGraw-Hill, New York
22. Someya Y, Sugahara Y, Shibata M (2005) J Appl Polym Sci 95:386
23. Herrera R, Franco L, Rodriguez-Galan A, Puiggali J (2002) J Polym Sci: Pt A: Polym Chem 40:4141
24. Tsutsumi C, Hayase N, Nakagawa K, Tanaka S, Miyahara Y (2003) Macromol Symp 197:431
25. Blumstein A (1965) J Polym Sci: Pt A: Polym Chem 3:2665
26. Biswas M, Ray SS (2001) Adv Polym Sci 155:167
27. Giannelis EP (1998) Appl Organomet Chem 12:675
28. Gilman JW (1999) Appl Clay Sci 15:31

Journal : 10924 | Dispatch : 1-8-2006 | Pages : 9
Article No. : 33 | ☐ LE | ☐ TYPESET
MS Code : 33 | ☑ CP | ☑ DISK